Does gravity affect the thermo-hydro-mechanical processes in a bentonite barrier?

María Victoria Villar[*], *Carlos* Gutiérrez-Álvarez, *Rubén Javier* Iglesias, *Pedro Luis* Martín

CIEMAT, Environment Department, 28040 Madrid, Spain

Abstract. To simulate in the laboratory the conditions of the buffer material in an underground repository for radioactive waste, three tests were performed in instrumented stainless steel cylindrical cells using compacted Wyoming-type bentonite. One of the cells was laid in vertical position and the other two stayed horizontal during operation, with the aim of checking if the layout of the cell affected the results obtained. At one end of the cells, a heater set at 90°C simulated the waste container. After two months of heating, hydration of the bentonite with a saline groundwater started through the surface of the cell opposite to the heater. One of the horizontal cells was dismantled right after the heating phase. After one year of hydration the other two cells were dismantled and the final physical state of the bentonite was analysed in terms of water content and dry density. It was checked that the spatial layout and hence, the effect of gravity, would only be to some extent noticeable if water vapour is involved, i.e. in those phases or processes in which water vapour movement is relevant (namely heating). In the liquid phase the effect of gravity on the water intake and water content and dry density distribution was not noticeable any more.

1 Introduction

Compacted bentonite will be one of the engineered barriers in the repository concept for spent nuclear fuel in Finland. In order to reduce conceptual and modelling uncertainties, POSIVA (the Finnish nuclear waste management organisation) is conducting research to assess the long-term behaviour of the buffer under variable water saturation conditions. The focus is on conditions that are specific to the future repository at Olkiluoto in terms of groundwater composition, bentonite type, and initial and boundary thermal and hydraulic conditions. Within this framework an experimental campaign is on-going at CIEMAT, in collaboration with Amphos 21, to study the evolution from 1 to 5 years of bentonite under thermal gradient. The experiments are performed using thermo-hydraulic (TH) cells with cylindrical bentonite samples and considering a thermal gradient and hydration with different synthetic groundwater on the cold side. The tests, which provide online results, are being dismantled after different periods of time to analyse the changes underwent by the bentonite. Although the focus is on the mineralogical alteration, a side aspect analysed was the possible effect of gravity on the processes involved. To this aim, tests were performed under identical conditions except for the cell layout, which was vertical in one of them and horizontal in the other two. One of the horizontal cells was heated but not hydrated, and this allowed also to tell apart the effect of the thermal and hydraulic gradients on the final physical state of the bentonite [1, 2].

2 Material

The material used in the TH tests was a Wyoming-type bentonite received from Posiva (Finland) in August 2016, with the characteristics reported in [3]. The characterisation performed at CIEMAT showed that it had a hygroscopic water content of 10% and a grain size smaller than 1 mm, with 85% of the particles being larger than 75 µm. Upon dispersion in water more than 86% of the particles were smaller than 2 µm. The density of solid particles is 2.78 g/cm^3 and the external specific surface area is 26 m^2/g. The mineralogical composition, determined by X-ray diffraction, includes 69% of montmorillonite, 14% of feldspars, 6% of quartz and smaller quantities of tridymite, cristobalite, calcite and gypsum. The cationic exchange capacity is 87 meq/100 g, with the main exchangeable cations being sodium (62 meq/100 g), calcium (29 meq/100 g), magnesium (8 meq/100 g) and potassium (3 meq/100 g). The main soluble ions are sulphate and sodium.

It was checked that the swelling pressure of this batch of Wyoming-type bentonite agreed with the values obtained for MX-80 bentonite powder compacted with its hygroscopic water content using deionised water as saturation fluid determined at CIEMAT [4]. The swelling pressure (P_s, MPa) could be related to final dry density (ρ_d, g/cm^3) through the following equation:

$$\ln P_s = 5.44\, \rho_d - 6.94 \quad (R^2=0.94,\ 33\ \text{values}) \qquad (1)$$

---

[*] Corresponding author: mv.villar@ciemat.es

The difference between experimental values and this fitting is, on average, 19%.

3 Experimental setup and methodology

The cylindrical TH cells were made out of stainless steel and had internal dimensions of 10x10 cm. The heating system for each cell consisted of a circular heater and corresponding monitoring and control systems. The heater was in direct contact with one of the lids of the cell. The opposite part of the cell included a cooling chamber where the cooling fluid was circulated. Each cell was instrumented with four RH/T capacitive transmitters, inserted at three different levels inside the bentonite block (at 2.5, 5.0 and 7.5 cm from the heater), and three total pressure sensors (PT) placed at the contact between the cell wall and the bentonite at the same levels as the RH/T sensors. Additionally, the external surface temperatures of the cells were measured by thermocouples stuck to them with adhesive film. In order to prevent external heat losses as much as possible, the cells were surrounded by a specific high-temperature thermal insulation material laterally and beneath. Hydration took place through a porous sinter in contact with the bentonite and was driven by gravity with a 1-m high water column from a 1-L glass flask. The composition of the hydration water reproduced that of a saline groundwater, mainly containing chloride, sodium and calcium [5]. The amount of water entering the system was measured by weighing the flask with a load cell.

The bentonite was mixed with deionised water to get a water content of 16-17% and after a stabilisation period it was uniaxially compacted inside the testing cell in five layers to a target dry density of 1.57 g/cm^3, corresponding to degrees of saturation of 60-63%. The tests consisted of an initial heating phase followed by a heating+hydration phase. The temperature of the cooling fluid circulating on top of the cells was 20°C and the heater temperature was 90°C.

Fig. 1. Appearance of cells C1h and C1 before and after being covered by the insulating material**.**

In contrast with cell C1, the layout of cells C1h and C1h_2 during operation was horizontal (Fig. 1). Test C1h was dismantled at the end of the heating phase, whereas the other two were dismantled after one year of hydration. The bentonite blocks were extracted by pressing with a piston once the lids of the cells had been removed. The blocks were measured, weighed and cut into five 2-cm thick sections. Each of these sections was subsampled for the different measurements. Namely, they were divided into internal and external zones, to check any potential "wall effect". Additionally, in the horizontal cells each section was also divided into up and down zones with respect to the position during operation, to check potential gravity effects. To determine the final water content of the subsamples they were dried at 110°C for 48 hours. The dry density of the speciments was determined by the mercury displacement method.

4 Results

4.1 Online results

Before starting the tests, the temperature inside the bentonite was 21°C and the relative humidity between 70 and 75%. There was an initial heating phase lasting between 2.1 and 2.9 months after which the relative humidity at different locations inside the bentonite was quasi-stabilised. The temperatures reached steady values in few hours. Away from the heater the difference between external and internal temperatures tended to be higher, likely as an effect of the cooling system (Fig. 2). The temperatures measured at the same distance from the heater either inside the bentonite by the capacitive sensors or on the surface of the cells with thermocouples were very similar in all the cells. Also, the thermal gradient generated from the heater towards the hydration surface was linear in the two kinds of cells, with values of 3.0-4.6°C/cm.
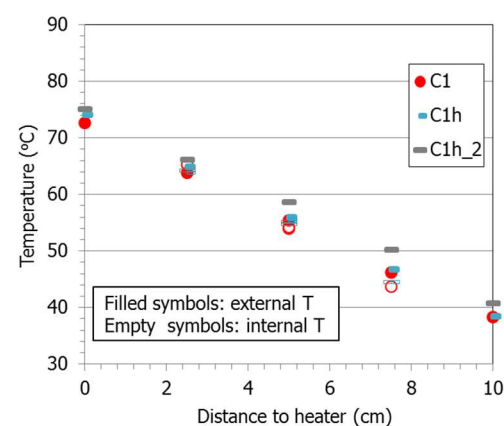

Fig. 2. Steady temperatures for the heating phase.

When the heater was switched on, the water vapour moved away from the heater, and initially the relative humidity recorded by all sensors increased. In the area opposite to the heater, the vapour pressure reached its saturation value at a lower temperature, and the sensor in this zone recorded 100% RH values until the end of the heating phase. In contrast, at 2.5 cm from the heater the relative humidity started to sharply decrease after the first day, indicating the drying of the material. In

the two middle sensors (5 cm from the heater), the relative humidity started to decrease after approximately two days, but did not reach values as low as for the bottom sensors. Hence, the RH values at the end of the heating phase showed a clear gradient, similar in the three tests, increasing from the heater towards the hydration surface (Fig. 3).
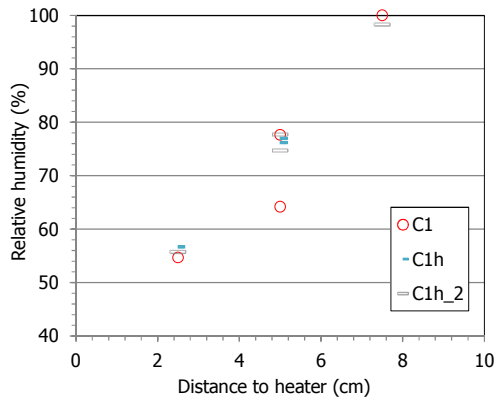

Fig. 3. Relative humidity at the end of the heating phase.

After the heating phase C1h was dismantled, whereas in cells C1 and C1h_2 the hydration circuit on the opposite side to the heater was opened. The temperatures were not affected by hydration and kept in the same values both externally and internally. Hence, at the end of the tests the thermal gradient along the two cells was similar. In fact, the power needed to keep a temperature of 90°C at the heater surface during the heating phase was between 4.1 and 4.6 W and this value did not change over the whole operation, despite the increase in water content and hence in thermal conductivity. The relative humidity inside the bentonite started to increase across the entire bentonite sample from the beginning of hydration and the two middle sensors recorded a RH of 100% after approximately two-three months. The lower sensor closest to the heater recorded a RH of 100% after approximately six months. Hence, at the end of the tests all the RH sensors were flooded, had condensed water in the filter or were located in areas where the vapour pressure reached its saturation value despite the high temperature. Hydration in cell C1h_2 was temporarily hindered by gas bubbles in the hydration system, which had to be periodically removed by opening the hydration circuit and extracting the air with a syringe. As a result, the final water intake of cell C1h_2 was slightly lower.

The radial pressure at the level of the sensor closest to the hydration surface started to increase shortly after hydration began and reached a final value of 3.8 MPa in the vertical cell and of 3.0 MPa in the horizontal one (Fig. 4). The pressure build up in the middle part of the bentonite block was slower in the horizontal cell, and the values at the end of the tests were also lower. At 2.5 cm from the heater no radial pressure was measured in any of the cells, although the relative humidity sensors in this area recorded at some moment RH=100% (meaning that the vapour pressure for the local temperature was reached inside the sensor's

filter). At the end of the tests (see next section) it was checked that the water content in this area was lower than the initial one, which explains why no radial pressure was developed in this area. The fact that the pressures were lower in the horizontal cell C1h_2, could be related to the lower water uptake measured in this cell. In fact, there were intermediate periods in the horizontal cell during which no water intake took place, and these coincided with decreases in the radial pressure.
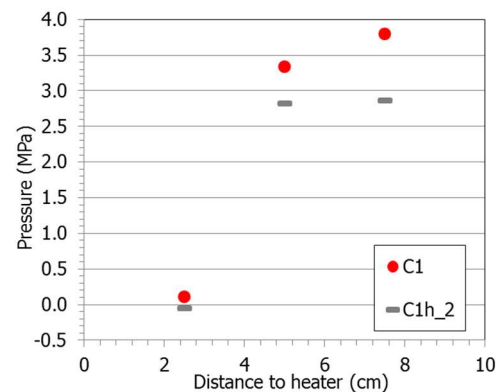

Fig. 4. Radial pressures at the end of the heating+hydration phase.

4.2 Postmortem results

At the end of the tests the blocks were extracted from the cells: they showed a consistent state, with no cracks (Fig. 5). The blocks were darker from the heater surface to the opposite side, indicating the increase in water content. The two hydrated blocks showed localised rust on the surface closest to the heater. The blocks were divided into 5 sections (coinciding approximately with the compaction layers), that were subsampled in external (e) and internal (i) samples, corresponding to the part in contact with the cell wall and the core one, and additionally, in the horizontal cells, up (U) and down (D) samples, corresponding to the upper and lower part of the cells according to their layout during operation.

Fig. 5. Appearance of the bentonite blocks of cells C1, C1h and C1h_2 (from left to right) once extracted (heater surface at the bottom, the five compaction layers are visible, as well as corrosion stains).

The comparison between the final water content and dry density of cells C1h and C1h_2 allows to tell apart the heating and hydration effects (Fig. 6, Fig. 7). The values plotted are the average of the external and internal subsamples, hence the difference between the upper and lower part of the cells is highlighted. Indeed

the water content increased from the heater towards the opposite surface and, in the case of cell C1h, the water content gradient along the block was linear and rather steep. In the two blocks the dry density was lower than the initial one in the 4 cm farthest from the heater, and higher than the initial one in the half block closest to the heater. The water content opposite to the heater was very high in the two cells. Although not shown in the Figure, in cell C1h the subsamples of the external part of the sections tended to have a slightly higher water content than those of the internal part, which could point out to some wall effect that was also seen close to the heater in cell C1h_2. Overall, all the sections of cell C1h tended to have higher water content and lower dry densities in the upper part, the difference between upper and lower parts being higher away from the heater. This distribution could indicate that water moved in the vapour phase from the heater to the opposite side and tended to concentrate in the upper part, revealing some gravity effect. After hydration (cell C1h_2) these differences between upper and lower parts attenuated, and even reversed in the half of the column farther from the heater. After hydration rhe water content was higher in the bottom part close to the hydration surface. The effect of gravity during saturation was opposite to that during heating: vapour would tend to concentrate upwards whereas liquid water will tend to concentrate downwards. Regarding dry density (Fig. 7), after hydration the upper parts had higher dry densities than the lower ones, except close to the heater. This would indicate that during saturation the upper part of the bentonite was compressed by the lower part which swelled more because its dry density was higher (as a result of heating) and because it received more water in the liquid phase. This would not happen close to the heater, an area which was far from saturation at the end of the experiment, explaining why close to the heater the dry density continued to be lower in the upper part after hydration.
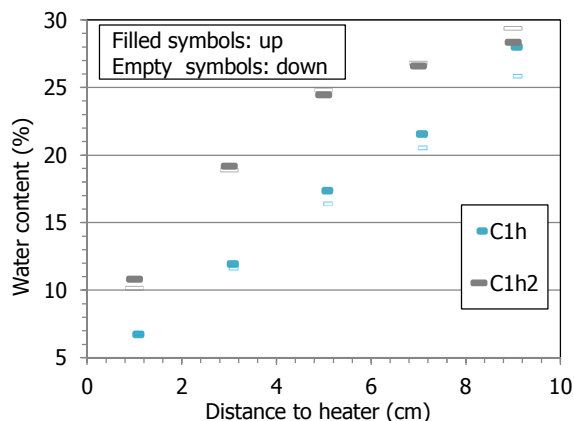

Fig. 6. Final water content for horizontal cell C1h (only heating) and C1h_2 (heating+hydration).

The spatial distribution at the end of hydration in tests C1 and C1h_2 (Fig. 8, Fig. 9) shows a slightly higher water content and degree of saturation (and lower dry density) at all locations in cell C1, the vertical one, but following the same patterns as in C1h_2, which is

remarkable and consistent with the pressure measurements. The average value of the water contents measured in all subsamples was 23% for cell C1 and 22% for cell C1h_2, which agrees with the lower water intake of the latter commented above.
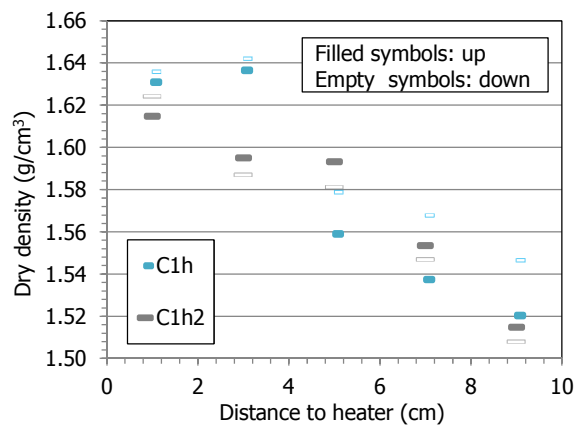

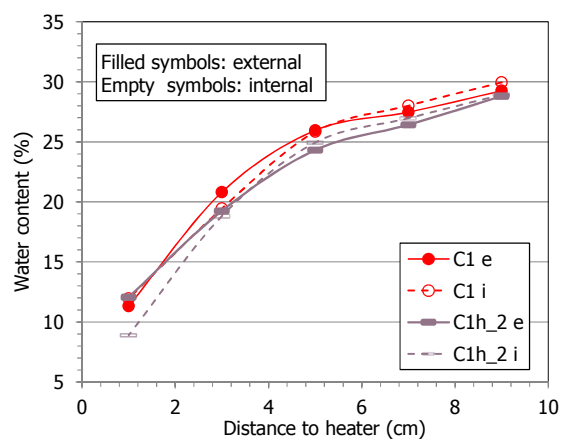**Fig. 7.** Final dry density for horizontal cell C1h (only heating) and C1h_2 (heating+hydration).

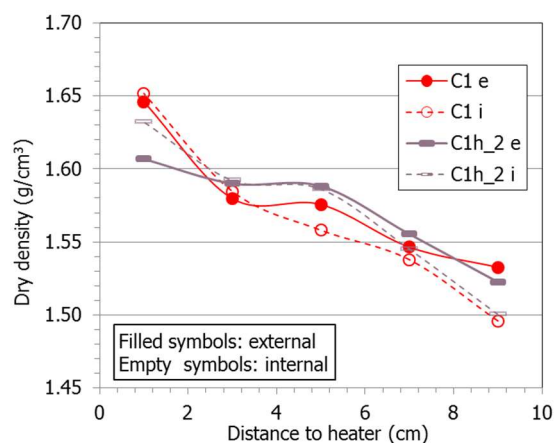**Fig. 8.** Final water content in cells C1 and C1h_2 (vertical / horizontal configuration).

Fig. 9. Final dry density in tests C1 and C1h_2 (vertical / horizontal configuration).

5 Summary and discussion

Three thermo-hydraulic tests were performed in stainless steel cylindrical cells using compacted Wyoming-type bentonite with an initial degree of saturation of 60-63%. One of the cells was laid in vertical position (C1) and the other two stayed horizontal during operation (C1h, C1h_2). Online and postmortem results allowed to analyse the processes taking place.

At one end of the cells, a heater was placed and set at 90°C. The temperatures inside the bentonite quickly stabilised, defining an almost linear thermal gradient across the length of the blocks. As a result of this gradient, vapour moved away from the heater and concentrated in the cooler areas. Hence, when one of the horizontal cells was dismantled after having reached hydraulic equilibrium under the thermal gradient imposed, it was observed that there was a gradient in the water content distribution, which increased from the heater towards the opposite end. It was also checked that, in its movement away from the heater, vapour tended to concentrate in the upper part of the block, where, for similar distances from the heater, the water content was slightly higher and the dry density slightly lower than at the bottom of the block.

Once the relative humidity inside the bentonite reached equilibrium –which took less than three months– hydration of the bentonite with saline water under low pressure started through the surface of the block opposite to the heater. During the hydration phase, the temperatures barely changed, but the relative humidity inside the bentonite gradually increased along the axis of the bentonite blocks. Although the water intake rate was initially similar for the two cells, it quickly became slower for the horizontal cell (C1h_2) as a result of air bubbles periodically blocking the hydration circuit. Therefore the final water intake of the vertical cell (C1) was slightly higher, but this difference is considered an artefact of the experimental configuration of the hydration system.

The pressure increase at the bentonite/cell interface (radial pressure) was in line with the RH changes and after one year of hydration was higher than 3 MPa in the more saturated parts of the two blocks, but lower in the case of the horizontal cell, which was related to the defective hydration commented above. These values are in the range of those expected for the MX-80 bentonite at dry densities of between 1.50 and 1.54 g/cm^3 (Fig. 9) saturated with deionised water, according to Eq. 1. Because the blocks were hydrated with saline water, lower values than those predicted by Eq. 1 (obtained with deionised water) could be foreseen. However, the final radial pressures were 0 at 2.5 cm from the heater. This is consistent with the final water content in this area, which was lower than the initial one, whereas the dry density was higher. Indeed no pressure would build up if no increase in water content took place. The increase of dry density would have been caused by the shrinkage of the bentonite block due to drying, which probably resulted in a bad contact between bentonite and pressure sensors.

Before the end of the tests all the RH sensors were saturated and/or had condensed water in the filter, including those closest to the heater where the vapour pressure reached the saturation value. Both the radial pressure values and the postmortem determinations showed that the parts of the blocks closest to the heater were far from saturation (the degrees of saturation measured were below 50%). This highlights the necessity of a rigorous evaluation of the values provided by sensors, through a correct calibration for different materials, depending on the water content, temperature and type of system (closed *vs.* opened).

Hydration proceeded for one year before the cells were dismantled. The comparison between the state of the horizontal cells after the heating phase (C1h) and after the hydration phase (C1h_2) showed that the differences between upper and lower parts of the block observed in the former had obliterated. In contrast, higher water contents were measured in the lower part of the coolest area after hydration, indicating that water in the liquid phase would tend to concentrate at the bottom. The movement of water vapour due exclusively to heating (despite the fact that the heater temperature was only 90°C) was so intense that the water content at the block side opposite to the heater was very similar to the water content reached in this area after one year of hydration. This indicates that the vapor phase is an important mechanism of water transport in a non-isothermal environment at sufficient temperature.

The two hydrated cells, in vertical and horizontal configuration, showed rather steep final gradients in water content and dry density, very similar in the case of water content and degree of saturation, only with slightly lower values for cell C1h_2, in agreement with the accidental lower total water intake of this cell.

6 Concluding remarks

The results obtained in this research seem to indicate that the effect of gravity, and hence the spatial layout, would only be to some extent noticeable when water vapour is involved, i.e. in those phases or processes in which water vapour movement is relevant, namely the first heating stages. Accordingly, the layout effect would not be relevant if the degree of saturation is very high and the effective porosity low, because this would hinder vapour movement. The saturation of the barrier in the liquid phase would be initially driven by the high suction of the bentonite, and factors such as localised water availability would be more influential on thermo-hydro-mechanical processes than the effect of gravity. Only in repository concepts, not reproduced in these tests, where the water availability is low or the temperatures very high (>100°C), the vapour concentration for long periods of time in the upper part of the barrier could give place to mineralogical and geochemical changes that should be separately analysed.

Another remarkable observation put forward in this research would be the efficiency of vapour as a water transport mechanism and as a factor in the development of heterogeneities in a non-isothermal environment at sufficient temperature.

References

1. M.V Villar, C. Gutiérrez-Álvarez, R.J. Iglesias, A.M. Melón, P.L. Martín, J.M. Barcala, J. Cuevas, A.I. Ruiz, A. Ortega, R. Fernández. Project Minalben. Final report on dismantling and postmortem analysis of cells C1 and C2. Technical Report CIEMAT/DMA/2G219/1/19. 89 pp. (2019)

2. M.V. Villar, C. Gutiérrez-Álvarez, R.J. Iglesias, P.L. Martín. Project MINALBEN. Report on dismantling of horizontal cells running for 1 year (C1h and C1h_2). Technical Report CIEMAT/DMA/2G219/2/20. 45 pp. (2020)

3. L. Kiviranta, S. Kumpulainen, X. Pintado, P. Karttunen, T. Schatz, T. Characterization of bentonite and clay materials 2012-2015. Posiva Working Report **2016-05**. 154 pp. (2018)

4. M.V. Villar. Long-term THM tests reports: Isothermal infiltration tests with materials from the HE-E. PEBS Deliverable 2.2-7.2. CIEMAT Technical Report CIEMAT/DMA/2G210/07/2013. 32 pp. (2013)

5. P. Hellä, P. Pitkänen, J. Löfman, S. Partamies, U. Vuorinen, P. Wersin. Safety Case for the Disposal of Spent Nuclear Fuel at Olkiluoto. Definition of Reference and Bounding Groundwaters, Buffer and Backfill Porewaters. POSIVA **2014-04**. (2014)